

Biogenic synthesis of copper oxide nanoparticles using aqueous rhizome extract of *Rubus ellipticus* for photocatalytic degradation of methylene blue

Gagan Shrestha* and Sabita Shrestha**

*Department of Chemistry, Amrit Science College, Lainchaur, Kathmandu, Nepal.

**Central Department of Chemistry, Tribhuvan University, Kirtipur, Kathmandu, Nepal.

Abstract: In this paper, we have reported the synthesis of CuO nanoparticles (CuO NPs) by cost effective and environmental friendly method using the rhizome extract of *Rubus ellipticus* for photocatalytic degradation of methylene blue. The biomolecules present in the extract acts as reducing agent and stabilizer for the synthesis of CuO NPs. The synthesized nanoparticles were characterized by using the different analytical instrument like UV-Visible spectrophotometer, XRD and FT-IR. The absorbance at 595 nm indicates the formation of CuO NPs which on annealing at 400 °C for four hours oxidizes and forms CuO NPs which shows maximum absorbance at 265 nm. XRD analysis confirms the formation of crystalline structured nanoparticles without any impurity. So formed nanoparticles were found to be of size 4.8 nm and 5.7 nm which was calculated by using Debye-Scherrer equation. The FTIR confirms the presence of various bioactive components, which acts as reducers and stabilizer. In addition, the photocatalytic degradation activity of the CuO NPs was studied for the degradation of the methylene blue in presence of sunlight. The catalytic activity was monitored using the UV-Visible spectrophotometer. It was found that the dye gradually degrade sunlight irradiation. This study highlights the application of CuO NPs for photocatalytic degradation of dye which can be extended for the waste water treatment.

Keywords: CuO nanoparticles; *Rubus ellipticus*; Biomolecules; Photocatalytic degradation.

Introduction

Nanotechnology deals with the design, characterization and application of nanomaterials. Nanomaterials has unique electronic, magnetic, optical, catalytic and medicinal features as compared to bulk materials, it is because nanomaterials have large surface to volume ratio, large surface energy and spatial arrangement¹. In recent years, the synthesis of metal oxide nanoparticles has gain great importance due to its versatile application namely electrochemistry, water splitting, solar cells, catalysis, gas sensor, high temperature superconductor, lithium ion electrode materials, field emission² etc. Among metal oxide

specifically cupric oxide nanoparticle (CuO NPs) has attracted the researcher as it has narrow band gap energy and can be used as p-type semiconductor. Copper oxide nanoparticles can be used in photo-thermal therapy as it exhibits similar properties to CuS³.

Mainly bottom-up and top-down approach is employed for the synthesis of nanoparticles. Bottom-up approach is easiest and cost effective as compared to top down method⁴. Many chemical and physical method are used for the synthesis of nanoparticles like precipitation method, decomposition method, plasma method, pulsed wire explosion method, sol-gel method, vapor deposition,

Author for correspondence: Sabita Shrestha, Central Department of Chemistry, Tribhuvan University, Kathmandu, Nepal.

Email: shresthasabita@hotmail.com

Received: 22 Feb 2022; First Review: 09 Mar 2022; Second Review: 24 Mar 2022; Accepted: 27 Mar 2022.

Doi: <https://doi.org/10.3126/sw.v15i15.45646>

electrochemical, radiolysis and so on⁵. Among these methods green synthesis is superior due to non-toxic and environmentally friendly.

Literatures showed that different plants are used for the synthesis of CuO NPs such as: *Rheum palmatum* L⁶, *Punicagranatum*⁷, *O.cochinchinese*⁸, *Gloriosa superba*⁹, *Thymus vulgaris*¹⁰, *Azadirachta indica*, *Hibiscus rosasnesis*, *Murraya koenigii*, *Moringa oleifera* and *Tamarindus indica*¹¹ etc. In the present work, Rhizome extract of *Rubus ellipticus* was used for synthesis of CuO NPs. *Rubus ellipticus* is Himalayan raspberry, which belonging to family Rosacea found in tropical and sub-tropical region of Nepal. It has bioactive compounds and used medicinally. It is used to treat fever, colic, cough, sore throat, vaginal/seminal discharge, polyuria and micturition during sleep¹². Environment pollution especially water pollution has attracted global focus. Photo-catalyst has been widely used for the treatment of polluted water mainly containing the organic dyes¹³. This type of degradation oxidizes complex organic compounds into small molecular inorganic substances, such as carbon dioxide and water, under sunlight. Methylene Blue (MB) is a thiazine dye (Figure 1). It is used to dye paper, silk etc. It has largely been used in human and veterinary medicine for several therapeutic and diagnostic procedures. The direct discharge of hazardous dyes from textile industries in water sources make water polluted. It can't be degraded through conventional water treatment processes due to its complex structures, hydrophilic nature, high stability against temperature, water, chemicals, etc. and it may cause substantial environmental pollution. Thus, there is a need to develop a suitable method for this pollutant dye treatment. In this study, photocatalytic degradation of methylene blue was done using the CuO NPs. Copper oxide nanoparticles was synthesized using aqueous rhizome extract of *Rubus ellipticus* which is clean, green and cost-effective method compared to chemical and physical method.

Experimental methods

Starting Materials: *Rubus ellipticus* rhizome was collected from hilly region of Nepal. It was dried and grinded to the

powder. Copper sulphate pentahydrate and methylene blue were from SD fine-CHEM LTD, assay 99.0%.

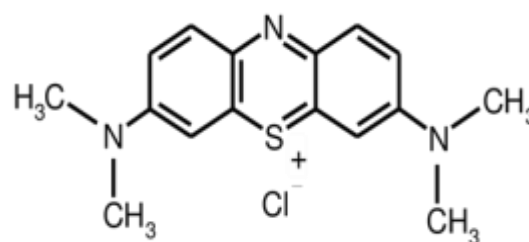


Figure 1: Structure of methylene blue

Preparation of plant extract: Aqueous extract of rhizome of *Rubus ellipticus* was prepared by heating (at 60°C) dried rhizome powder (10 g) with distilled water (100 mL) for about 30 mins. Then it was filtered and stored in freeze for further use.

Synthesis of CuO nanoparticles: In typical synthesis of CuO NPs, CuSO₄.5H₂O (0.1 M, 80 mL) and rhizome extract (20 mL) was stirred at 400 rpm for 3 hours maintaining temperature 80 °C. Then it was centrifuged at 4000 rpm for 15 minutes and precipitated was washed several times with distilled water. Finally, the precipitated was calcined at 400 °C for 4 hours.

Characterization: The prepared CuO NPs was characterized by using UV-Visible spectrometer (SPECTRO UV-2510TS) Fourier Transform Infrared spectrometer (Shimadzu, Tracer 100). Crystalline structure of CuO NPs was studied by X-ray diffraction XRD, Rigaku Japan (using Cu ka) $\lambda = 1.54 \text{ \AA}$ radiation and Bragg angle (2θ) in the range of 5° to 90°. The size of crystalline structure was calculated by Debye-Scherrer equation:

$$D = 0.94 \lambda / \beta \cos \theta$$

Where, D = Particle size, λ = Wavelength, β = Full width half maximum and θ = Angle of diffraction

Photocatalytic degradation of dye: The photo degradation of Methylene Blue (MB) in presence of CuO NPs was studied spectrophotometrically. For this, a mixture containing MB (10^{-3} M, 300 μ L), 1 mg of CuO NPs and distilled water (20 mL) was taken. Then it was irradiated to sunlight and absorbance was noted at regular interval of

time. The colour of the mixture faded gradually indicating that degradation had occurred.

Results and discussion

UV-Vis spectral study: UV-Visible spectroscopy is one of the important characterization techniques to study the synthesized nanoparticles. UV-Vis spectral study was done for Cu NPs as well as CuO NPS. The formation of Cu NPs and CuO NPS from rhizome extract of *Rubus ellipticus* was initially monitored by color change and confirmed by UV-Vis absorption study.

Formation of Cu NPs: Copper nanoparticles typically exhibit absorbance around 550-700 nm in UV-Vis spectrum¹⁴. UV-Vis spectrum of CuNPs synthesized in this

strongly depend on various factors such as size, shape and monodispersity of the NPs, as well as the composition of the surrounding media and interactions between stabilizing ligands and the NPs¹⁵.

Formation of CuO NPs: Bordbar, et al., reported the absorbance of CuO NPS within the range of 250-300 nm¹⁶. UV-Vis spectrum of CuO NPs synthesized in this work was found at 265 nm shown in Figure 2 (b) indicating the formation of CuO nanoparticles¹⁶. The color of CuO NPs was black. Hence, confirms the cupric oxide nanoparticle rather than cuprous oxide nanoparticles. Figure 2 (c) represents the UV-Vis spectrum of root extract of *Rubus ellipticus* the absorbance was seen around 350-400 nm. As we compared the Figures 2 (a), (b) and (c) different

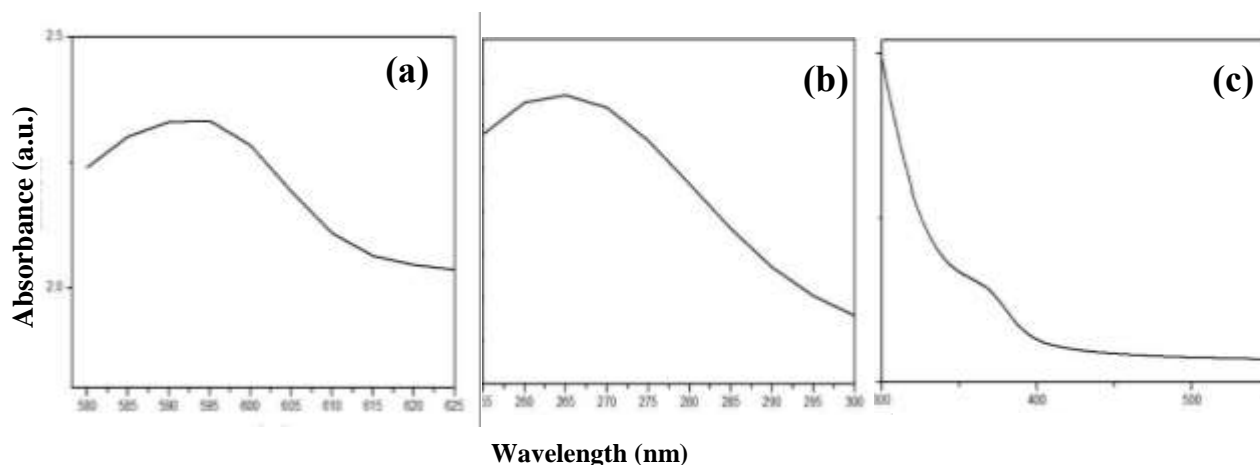


Figure 2: UV-Vis Spectra of (a) Cu NPs (b) CuONPs (c) Rhizome Extract of *Rubus ellipticus*

work was found around wavelength 595 nm as shown in Figure 2 (a). The color of solution changes from light brown to dark and then black. The change in color is due to the surface plasmon resonance phenomenon which confirms the formation of Cu NP⁶. Many metals can be treated as free-electron system. Such metal are called plasma and contains equal number of positive ion fixed in position and free conduction electron which are free and mobile. Under the irradiation of an electromagnetic wave, the free electrons are driven by the electric field to oscillate coherently. These collective oscillations of the free electrons are called plasmons. These plasmons under certain conditions react with visible light in a phenomenon called surface plasmon resonance (SPR). The position, shape and intensity of the surface plasmon resonance

peaks at different wavelength were obtained hence, prove the formation of intended nanoparticles.

The reducing agent present in the biomolecules of rhizome extract of *Rubus ellipticus* was responsible for the formation of nanoparticles.



Optical band gap calculation: Optical band gap is measure of energy on transition between valance bands to conduction band. An excitation occurs when the semiconductor absorbs a photon, so photon is a threshold for excitation to occur in semiconductor. It can be of direct and indirect depending on the momentum of valance and conduction band. If the momentums are same then it is direct optical band gap otherwise it in indirect optical band

gap. The optical band gap can be calculated by using Tauc's relation:

$$\alpha h\nu = A (h\nu - E_g)^n$$

where, A= Absorbance coefficient, h = Planck's constant, ν = frequency of incident photon, E_g = optical band gap, n = index that depends upon nature of electronic transition responsible for optical absorbance.

Figures 3 (a) and (b) represent the optical band gap of Cu NPs and CuO NPs respectively. The optical band gap was found to be 1.99 and 4.26 eV for Cu NPs and CuO NPs respectively. The band energy was found to be slightly higher than the recorded value because of band gap confinement effect which means that band gap of semiconductors increases with decrease in the size of nanoparticles semiconductor¹⁷.

XRD analysis: The X- ray diffraction pattern of synthesized CuO NPs was shown in Fig. 4. The XRD pattern reveals the orientation and crystalline structure of the synthesized nanoparticles. In this study, the detected peaks were good agreement with those of powder CuO obtained from the International Center of Diffraction. Data card (JCPDS-45-0937) confirming the formation of a crystalline structure¹⁸. No extra diffraction peaks of other phases were detected, indicating the phase purity of CuO NPs.

The average crystallite size of the synthesized CuO NPs was calculated using Debye-Scherrer equation.

The FWHM of two highest peaks indexed as 002 and 200 were found to be 0.31232 and 0.38269 and Bragg's angle were 35.5° and 38.7° respectively. Thus, calculated particle size was found to be 4.8 nm and 5.7 nm.

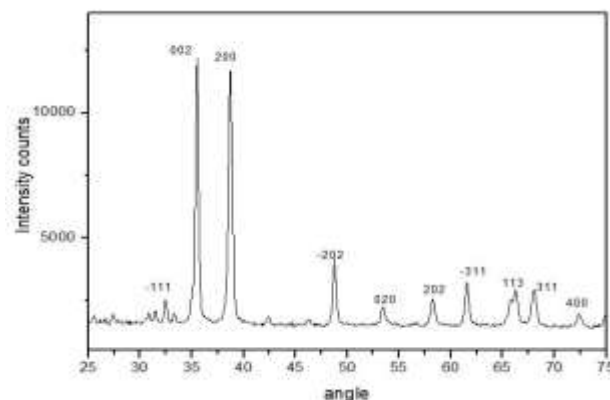


Figure 4: XRD Pattern of CuO NPs

Fourier Transform Infrared Spectroscopy: Figure 5 (a) represents the FTIR spectrum of rhizome extract which confirms the presence of various biomolecules, which display the numbers of peaks. Strong and broad peak at 3296 cm^{-1} attributes the OH group of phenol and NH of amine 1640 cm^{-1} signifies C-OH of protein⁷.

Figure 5 (b) shows the Fourier transform infrared spectroscopy (FTIR) peaks of CuO NPs at 509, 516, 520, 1015, 1643 and 3278 cm^{-1} . Here in the case of synthesized

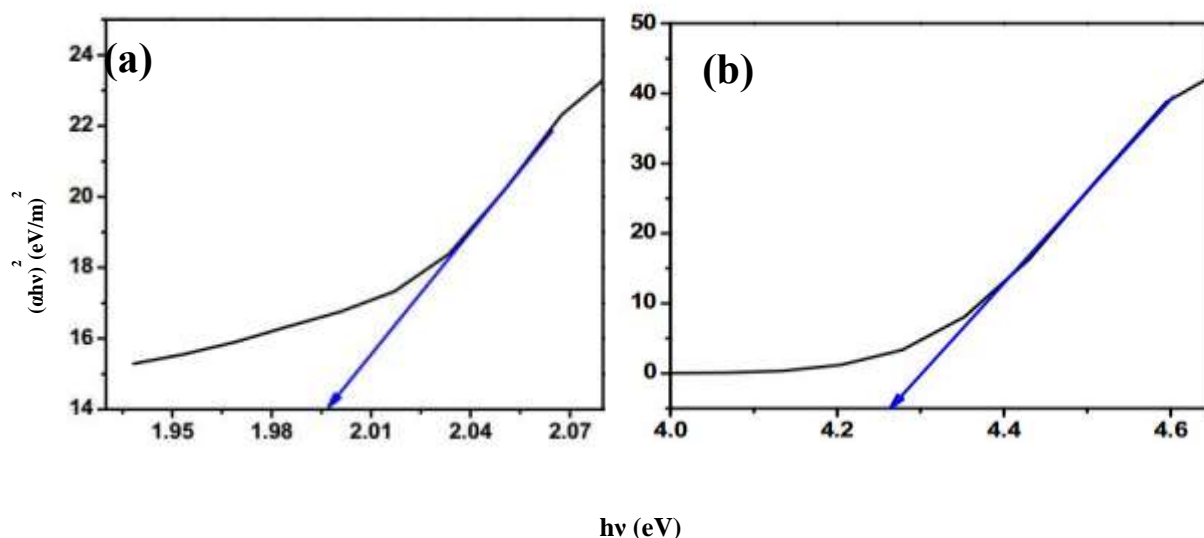


Figure 3: Optical Band Gap of (a) Cu NPs (b) CuO NPS

nanoparticles, the resulting nanoparticles were dried in a hot air oven, due to which intensity of peaks of OH and NH were decreased.

The peak at 1,070 cm^{-1} indicated the presence of C–O stretching frequency. The peak at 1643 cm^{-1} represented the unreacted ketone group. New peaks arise around 509-520 cm^{-1} indicated the Cu–O stretching¹⁹. Peaks at around 509-520 cm^{-1} were absent in the IR spectrum of plant extract whereas present in IR spectrum of CuO NPs hence, confirmed the formation of CuO NPs.

Photocatalytic Degradation of Methylene Blue: The photocatalytic activity of green synthesized CuO NPs was studied for the degradation of methylene blue (MB) by sunlight irradiation. Figure 6 reflects the mechanism of catalytic degradation²⁰ of MB by CuO nano-catalyst.

The light induces the electron hole pair in CuO. The electrons get transmitted to the conduction band (CB) from

valence band (VB). The hole remains at VB. After separation of electrons and holes, the dissolved oxygen (O_2) adsorbed on CuO NPs surface will react with photo-induced electrons to form superoxide radical ($\text{O}_2^{\cdot-}$). The hydroxyl ions (OH^-) will be oxidized into hydroxyl radicals (OH^\cdot) by photo-induced holes. Finally, the dye molecules are decomposed into simple organics by the continuous generated reactive oxidation species and further converted into CO_2 and H_2O ²¹.

The methylene blue shows λ_{max} around 590 nm. The absorbance was decreased gradually with the certain interval of time during irradiation as shown in Figure 7 (a). The rate of degradation of MB increases with increase in irradiation time. The rate of degradation vs time has been shown in Figure 7 (b).

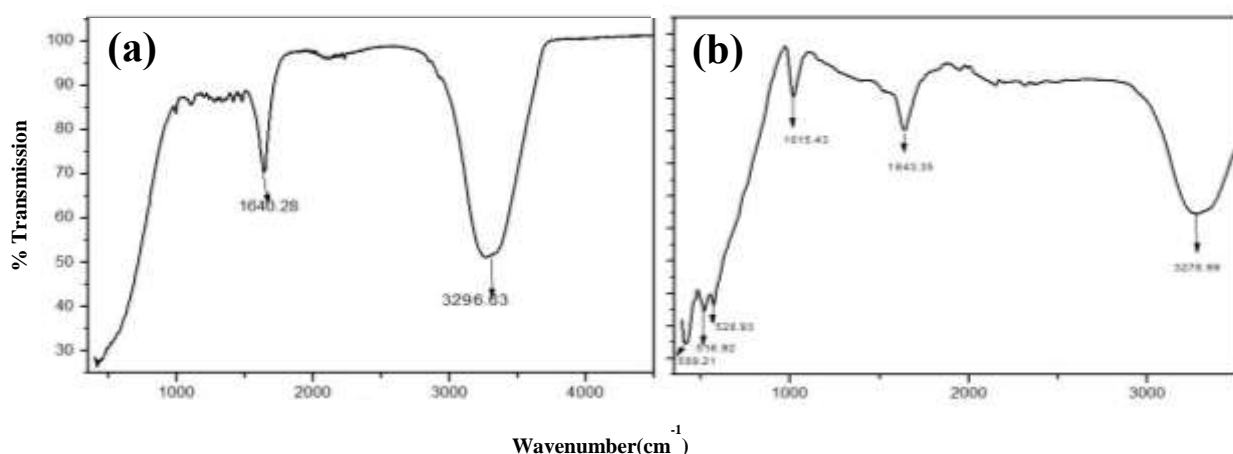


Figure 5: FTIR Spectra (a) Plant Extract (b) CuO NPs

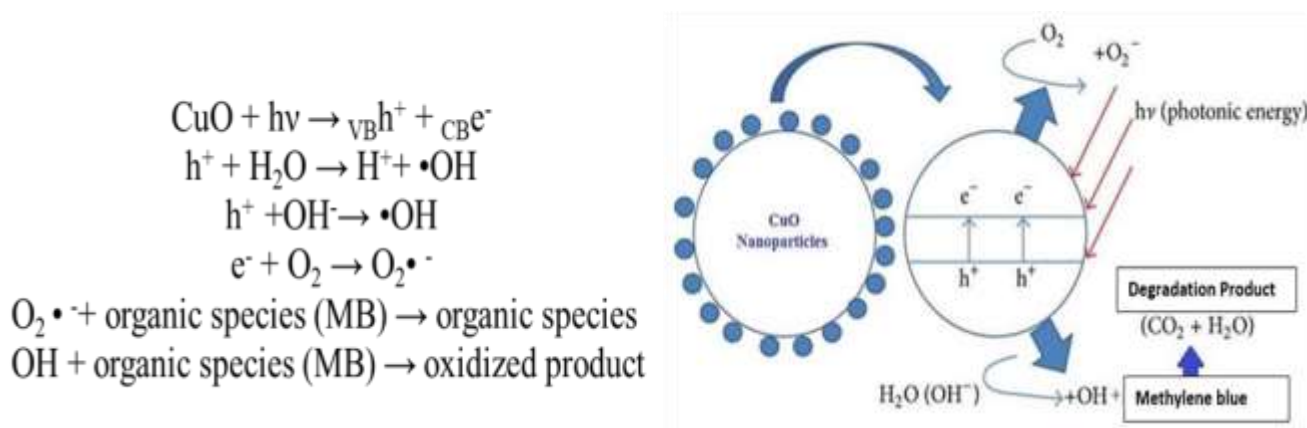


Figure 6: Mechanism of photocatalytic degradation

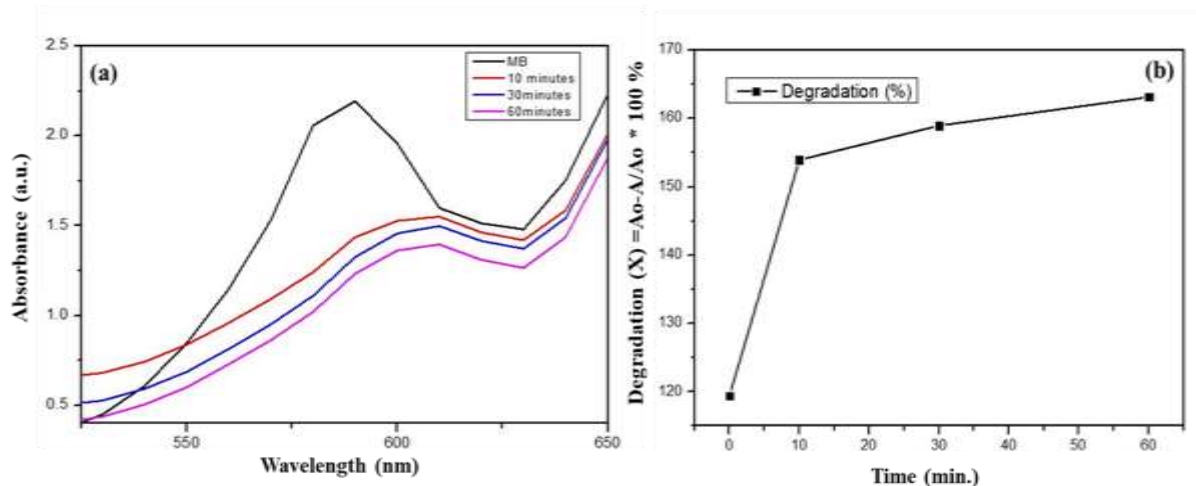


Figure 7: (a) Photocatalytic degradation of methylene blue (b) Dye degradation vs Time

Conclusions

The formation of nanoparticles was confirmed by the UV-Visible spectrophotometer. The UV-spectrum of plant extract showed maximum absorbance at about 370 nm. Similarly, λ_{\max} of Cu NPs and CuO NPs showed at 595 nm and 265 nm respectively. The XRD pattern confirms the crystallinity and purity of nanoparticles. The particle size was calculated by Debye-Scherrer's equation. The particle size of two prominent peaks were found to be 4.8 nm and 5.7 nm. The FTIR spectrum showed various biomolecules that helped in the formation of nanoparticles. The Cu-O stretching was seen at 509-520 cm^{-1} . The synthesized nanoparticles is found to be excellent photo-catalyst for the degradation of methylene blue dye. The proposed mechanism was attributed as charge transfer process where oxidation and reduction occur and finally forms simple degraded product they are H_2O and CO_2 . Thus, so formed nanoparticle can be used as a waste water treatment agent .

Acknowledgements

We would like to acknowledge Central Department of Chemistry, T. U. for recording FTIR, Chemistry Department, Amrit Science Campus for UV-V is spectra and Dr. Suresh Dhungel, Nepal Academy of Science and Technology for powder XRD.

References

1. Aminuzzaman, M., Kai, L. and Liang, W. 2017. Green synthesis of copper oxide (CuO) nanoparticles using banana peel extract and their photocatalytic activities. *American Institute of Physics*. **6**: 1-5
2. Li, et al. 2012. Fabrication and photocatalytic property of CuO nanosheet via a facile solution route. *Cryst.Res.Technol.* **47**: 1140-1147.
3. Sathyamoorthy, R. and Mageshwari. 2013. Synthesis of hierarchical CuO microspheres: Photocatalytic and antibacterial activities. *Physica E*. **47**: 157-161.
4. Li, et al. 2014. Synthesis and photocatalytic properties of CuO nanostructure. *Journal of Nanoscience and Technology*. **14**: 3428-3432.
5. Devi, S. H. and Singh, D. T. 2014. Synthesis of copper oxide nanoparticles by a novel method and its application in the degradation of methyl orange. *Advance in Electronic and Electric Engineering*. **4**: 83-88.
6. Bordbar, M., Sharifi, Z. and Khodadadi, B. 2016. Green synthesis of copper oxidenanoparticles/clinoptilolite using *Rheum palmatum* L root extract high catalytic activity for reduction of 4-nitrophenol, rhodamine B and methylene blue. *J Sol -Gel Technol.* **81**: 724-733.
7. Ghidan, Y., Al-Antary, T. and Awwad, M. 2016. Green synthesis of copper oxide nanoparticles using Punica granatu, peel extract: effect on green peach aphid. *Environmental Nanotechnology: Monitoring and mangae ment*. **6**: 95-98.
8. Gnanavel, V., Palanichamy, V. and Roopsn, S. 2017. Biosynthesis and characterization of copper oxide nanoparticles and its anticancer activity on human colon cancer cell line (HCT-116). *Journal of Photochemistry and Photobiology B: Biology*. **1**: 133-138.
9. Naika, et al. 2015. Green synthesis of CuO nanoparticles using *Gloriosa suoerba* L extract and antimicrobial activity. *J. Taibah Univ. Sci.* **9**: 7-12.
10. Nasrollahzadeh, M. and Sajadhi, S. 2015. Green synthesis of CuO nanoparticles by aqueous extract of *Gundelia tournefortii* and evolution of their catalytic activity for the synthesis of N-monosubstituted ureas and reduction of 4- nitrophenol. *J. Colloid Interface Sci.* **455**: 245-253.

11. Rehana, et al. 2017. Evolution of antioxidant and anticancer activity of copper oxide nanoparticles synthesized using medicinally important plant extract. *Biomedicine and Pharmacotherapy*. **89**: 1067-1077.
12. Saklani, et al. 2012. Antimicrobial activity, nutritional profile and phytochemical screening of wild edible fruit of *Rubus ellipticus*. *Int. J. Med Arom Plants*. **2**: 269-274.
13. Sorbium, et. al. 2018 .Green synthesis of zinc oxide and copper oxide nanoparticles using aqueous extract of oak frut hull (jaft) and comparing their photocatalytic degradation of basic violet-3 . *International Journal of Environmental Research*. **12(1)**: 29-37.
14. Dash, A. R., Raj, P. C. and Gedanken, A. 1998. Synthesis, characterization and properties of metallic copper nanoparticle. *Chem Mater*. **10**: 1446-1452.
15. Honary, et al. 2012. Green synthesis of copper oxide nanoparticles using penicillium aurantiogriseum, penicillium citrinum and penicillium waksman. *Digest Journal of Nanomaterials and Biostructure*. **7**: 999-1005.
16. Bordbar, M., Sharifi-Zarchi, Z. and Khodadadi, B. 2016. Green synthesis of copper oxide nanoparticles/clinoptilolite using Rheum palmatum L. root extract :high catalytic activity for reduction of 4-nitro phenol, rhodamine B, and methylene blue. *Sol-Gel Sci Technol*. **81**: 724-733.
17. Rafea, M. A. and Roushdy, N. 2008. Determination of the optical band gap for amorphous and nanocrystalline copper oxide thin films prepared by SILAR technique. *Journal of Physics D: App Phys*. **41(1)**: 1-6.
18. Abboud, et. al. 2014. Biosynthesis, characterization and antimicrobial activity of copperoxide nanoparticle (CuONPs) produced using brown algae extract (*Bifurcana bifurcata*). *Applied Nanoscience*. **4**: 571-576.
19. Sutradhar, P., Saha, M. and Maiti, D. 2014. Microwave synthesis of copper oxide nanoparticles using tea leaf and coffee powder extracts and its antibacterial activity. *J. Nanostruct Chem*. **4**: 86.
20. Devi, H. S. and Singh, T. D. 2014. Synthesis of copper oxide nanoparticles by novel method and its application in degradation of methyl orange. *Advance in Electronic and Electric Engineering*. **4(1)**: 83-88.
21. Ijaz, et. al. 2017. Green synthesis of copper oxide nanoparticles using *Abutilon indicum* leaf extract: Antimicrobial, antioxidant and photocatalytic dye degradation activities. *Tropical Journal of Pharmaceutical Research*. **16(4)**: 743-753.

